

XV-15 Tiltrotor Low Noise Terminal Area Operations

David A. Conner
Research Engineer
U.S. Army Joint Research Programs Office/AFDD
Hampton, VA

Michael A. Marcolini
Senior Research Engineer
NASA Langley Research Center
Hampton, VA

Bryan D. Edwards and John T. Brieger
Senior Engineer Specialists
Bell Helicopter Textron, Inc.
Fort Worth, TX

Abstract

Acoustic data have been acquired for the XV-15 tiltrotor aircraft performing a variety of terminal area operating procedures. This joint NASA/Bell/Army test program was conducted in two phases. During Phase 1 the XV-15 was flown over a linear array of microphones, deployed perpendicular to the flight path, at a number of fixed operating conditions. This documented the relative noise differences between the various conditions. During Phase 2 the microphone array was deployed over a large area to directly measure the noise footprint produced during realistic approach and departure procedures. The XV-15 flew approach profiles that culminated in IGE hover over a landing pad, then takeoffs from the hover condition back out over the microphone array. Results from Phase 1 identify noise differences between selected operating conditions, while those from Phase 2 identify differences in noise footprints between takeoff and approach conditions and changes in noise footprint due to variation in approach procedures.

Notation

BHTI Bell Helicopter Textron, Inc.
IGE In Ground Effect
 L_A A-weighted Sound Pressure Level, dBA

L_{Amax} Maximum L_A obtained during a flyover, dBA
 L_{AE} Sound Exposure Level (SEL), dB
 L_{DN} Day-Night Average Sound Level, dB
OASPL Overall Sound Pressure Level, dB (re 20 μ Pa)
 $OASPL_{max}$ Maximum OASPL obtained during a flyover, dB
X Coordinate along flight path direction, positive in the aircraft's direction of flight, ft.
Y Coordinate perpendicular to flight path direction, positive to the port side of the aircraft, ft.
Z Coordinate in vertical direction, positive up, ft.

Introduction

An increasing number of U.S. airports, particularly in the Northeast, are rapidly approaching (or have already reached) their saturation point with regard to the maximum number of daily aircraft operations. Many of these valuable slots are used up by commuter aircraft (Ref. 1) flying fairly short routes with relatively few passengers, which significantly limits the total number of passengers that can use that airport each day. Tiltrotor aircraft, with their unique capability to take off and land vertically yet still fly like an airplane during cruise, provide a potential alternate means of transportation that could link major cities, thus alleviating some of the demand on airports. Research on tiltrotor aircraft has been conducted for many years using such vehicles as the XV-3 and the XV-15, among others. More recently, the Navy has begun procurement of the V-22 Osprey to utilize the capabilities of the tiltrotor for military

applications. However, noise generated by such large tiltrotor aircraft is a potential barrier issue for civil market penetration. The Civil Tiltrotor Development Advisory Committee (CTRDAC), in a report to Congress, stated that reduction of external noise is a major requirement for community acceptance of civil tiltrotor aircraft (Ref. 2). George et al. (Ref. 3) reviewed tiltrotor aeroacoustics, describing the primary noise sources, as well as reviewing the experimental and analytical state-of-the-art.

The predominant tiltrotor research aircraft of the 1970's and 1980's was the XV-15. Two of these aircraft were constructed as a joint NASA/Army/Bell venture, and a great deal of acoustic testing has been accomplished using these vehicles. Lee and Mosher (Ref. 4), in a test of an XV-15 in the NASA Ames 40x80 Foot Wind Tunnel, showed significant variation (10-15 dB) in noise level as a function of nacelle tilt, but only at four fixed measurement locations. Both Maisel and Harris (Ref. 5) and Conner and Wellman (Ref. 6) conducted XV-15 flight tests that successfully mapped the aircraft directivity during hover for two different rotor blade sets. Brieger, Maisel, and Gerdes (Ref. 7) acquired acoustic data during level flight, ascent, and descent operating conditions. The results of Reference 7 showed significant variation in noise generation with nacelle tilt, but since acoustic data were only acquired at two sideline angles to each side of the aircraft, directivity information was again limited. Edwards (Ref. 8), in another XV-15 acoustics flight test, acquired data using a large array for the purposes of obtaining noise footprint data, but only for a limited test matrix. In a joint NASA/Army/BHTI test of a model tiltrotor in the 14- by 22-Foot Subsonic Tunnel at the NASA Langley Research Center, Marcolini et al. (Ref. 9) again showed significant variations in both noise level and directivity as a function of rotor operating condition.

One means of reducing the noise produced by tiltrotor aircraft is by design and installation of quieter rotors. However, this requires design/cost tradeoffs and a significant lead time. A second approach is to make use of the nacelle tilt capability, which allows the tiltrotor to fly a specified flight path for a number of different rotor operating conditions.

To address this second approach, NASA, BHTI, and the Army conducted a flight test of the XV-15 operated with the standard metal rotor blades in October-November 1995. Results from measurements of noise directivity at fixed operating conditions, as well as ground footprint measurements of realistic approaches and departures are presented. These results document

the variation in tiltrotor noise due to changes in operating condition, and indicate the potential for significant noise reduction using the unique tiltrotor capability of nacelle tilt. In addition, these results can be used in conjunction with cockpit display and handling qualities research to develop noise abatement flight procedures that are safe, quiet, and easy to fly.

Experimental Setup

This flight test was performed in a rural area near the town of Waxahachie, Texas, on a tract of land which had been the site of the former Superconducting Super Collider (SSC). The site is sufficiently remote that the ambient noise levels were low (25 to 40 dBA), yet near enough to the Dallas-Fort Worth area to allow flight operations to be based out of BHTI's Arlington flight facility. The terrain is generally flat with few trees. During the test period, the ground was covered with relatively short, mowed grass.

Test Program

The flight test was conducted in two phases. In Phase 1 the XV-15 was flown over a linear array of microphones, deployed perpendicular to the flight path, at a number of fixed nacelle angle and airspeed combinations for several glideslopes. This documented the relative noise differences between the various conditions. During Phase 2 a microphone array was deployed over a large area to directly measure the noise footprint produced during actual approach and departure procedures. The XV-15 flew typical approach profiles that culminated in IGE hovers over a landing pad, then typical takeoffs from the hover conditions back over the microphone array.

Test Aircraft

The XV-15 tiltrotor aircraft used for this test (Figure 1) was built by Bell Helicopter Textron, Inc. (BHTI), as a proof of concept aircraft and technology demonstrator whose first flight was in May 1977. The XV-15 has two 25-foot diameter rotors mounted on pivoting nacelles which are located on the wing tips. Each nacelle houses a main transmission and a Lycoming T-53 turboshaft engine capable of generating 1800 shaft horsepower. The nacelles are tilted near the vertical position (90° nacelle angle) for takeoffs and landings and rotated to the horizontal (0° nacelle angle) for cruising flight. Each rotor has three highly twisted, square-tip, stainless steel blades. These typically operate at 589 RPM during hover and transitional flight modes, and at 517 RPM during



Figure 1. XV-15 tiltrotor aircraft hovering over hover pad at the test site near Waxahachie, Texas.

cruise, which correspond to 98% and 86% of rotor design speed. The wings have a 6.5 degree forward sweep to provide clearance for rotor flapping. A more detailed description of the XV-15 aircraft is available in Reference 10.

During this test, the nominal vehicle takeoff gross weight was 13,800 pounds. The vehicle was operated by BHTI under contract to NASA. BHTI furnished research pilots, flight test engineers, ground crew personnel, and other necessary support personnel for operation and maintenance of the aircraft and on-board data acquisition system. More than 100 aircraft state parameters were measured and recorded on magnetic tape. Transducers included attitude and rate gyros, strain gauges, temperature sensors, accelerometers, and control position sensors.

The XV-15 flight envelope, shown in Figure 2, illustrates combinations of nacelle angles and airspeeds necessary to achieve stabilized flight. It should be noted that a fairly broad range of nacelle angles and airspeeds is possible within this operating envelope. The acoustic effects of avoiding certain portions of this range can guide flight operations of the XV-15 (and presumably other tiltrotor aircraft) in minimizing external noise. The present test was designed to define and quantify these effects, with particular emphasis on approach conditions.

Aircraft Tracking and Guidance

Aircraft tracking was provided by personnel from the Moffett Range Systems Branch (MRSB) of the NASA Ames Research Center using the Precision Automated Tracking System (PATs). The PATs system uses a pulsed laser beam with a 100 Hz pulse rate to measure

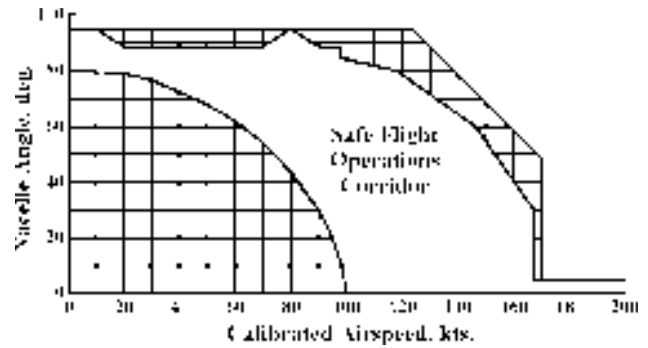


Figure 2. XV-15 flight envelope.

the position of the aircraft within 0.1 mrad in azimuth and elevation and ± 1 ft in range. These measurements are then converted to absolute X, Y, and Z coordinates for the aircraft with respect to the acoustic reference location. Along with tracking aircraft position, the MRSB's Instrument Positioning System (IPS) was used to provide flight path guidance information to the pilots. The IPS system compares the actual aircraft position to a preselected desired flight profile, and transmits an error signal to a traditional Instrument Landing System (ILS) receiver and display installed on board the XV-15. This system provides real-time feedback to the pilots regarding their position with respect to the desired flight profile. In addition to the IPS, three 1000 watt metal halide lights with parabolic reflectors oriented towards the aircraft when inbound were deployed along the desired flight path approximately 25 feet above ground level at both ends and at the center of the test range property. These lights were visible to the pilots several miles out and provided very useful visual cues of the desired flight path.

Meteorological Instrumentation

A tethered weather balloon system and a weather profiler system were used to acquire weather information. The tethered weather balloon system consisted of an electric winch-controlled, tethered, helium-filled balloon, an instrument/telemetry pod, a ground-based receiver/data-controller, and a ground-based support computer. Profiles of temperature, relative humidity, wind speed, and wind direction up to 400-ft altitude were acquired continuously during each flight test period. An example of these data acquired during a typical flight test period are presented in Figure 3. The weather profiler system consisted of a 10-meter tower with 10 temperature sensors, five anemometers, and three wind direction sensors. The weather profiler was used to obtain detailed weather information near the ground. Weather data from both systems were acquired at a rate of at least six points

per minute, displayed in real time, and recorded, along with satellite time code, on a magnetic disk.

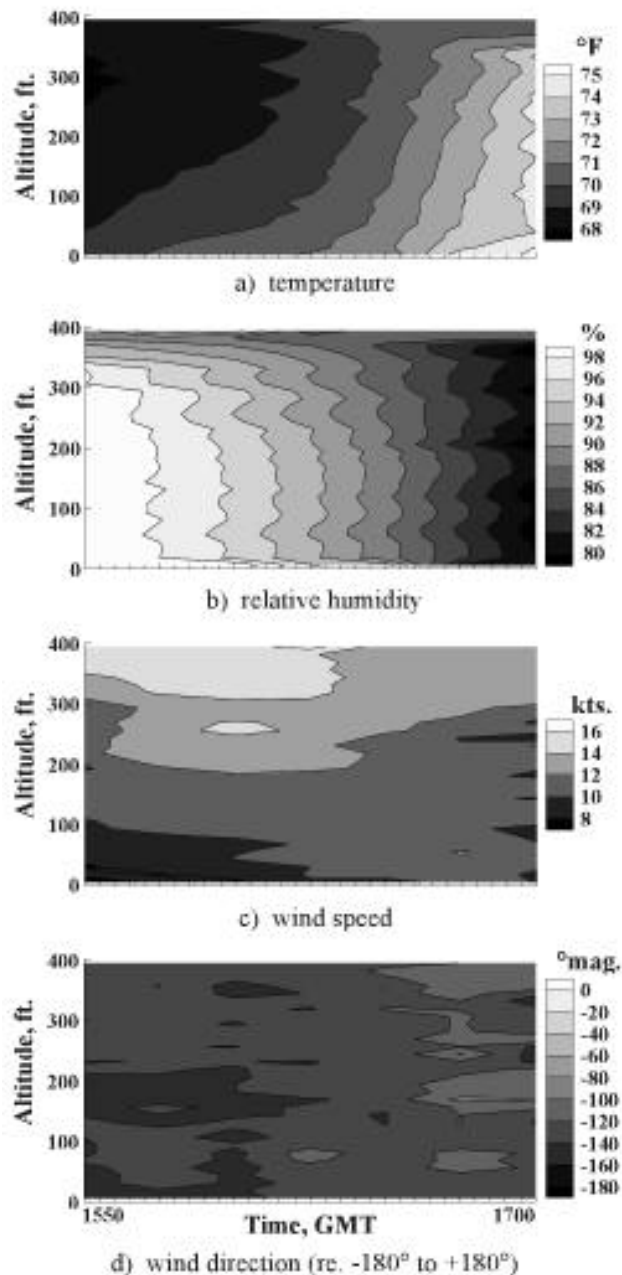


Figure 3. Weather profiles for typical test period.

Acoustic Instrumentation

Two completely different microphone array configurations were used to acquire acoustic data during this flight test program. Both arrays primarily used NASA Langley's digital acoustic recording system. With this system the microphone signals are digitized at the microphone, transmitted via cables to a data van,

multiplexed with time and run information, and then recorded on 8-mm tape (Ref. 11). A maximum of three Langley acoustic data vans were deployed, and each data van could handle a maximum of 10 microphone systems. The linear microphone array shown in Figure 4 was used during Phase 1 for steady state flight operations, while the large microphone array shown in Figure 5 was used during Phase 2 for steady state and non-steady state flight operations.

The linear microphone array used in Phase 1 consisted of 20 ground board mounted microphones arranged in the shape of a "T", as shown in Figure 4, with 17 microphones forming the top of the "T" and the remaining three microphones making up the stem. The centerline microphone, which was common to both the top and the stem of the "T", was defined as the reference microphone and was the origin of the coordinate system ($X = Y = Z = 0$) used during Phase 1 testing. The aircraft flight track was perpendicular to the top of the "T", passing directly over the stem of the "T" and the reference microphone, from $-X$ to $+X$, as shown in the figure. The unequal spacing of the 17 microphones lying perpendicular to the flight track was designed to provide a 10° angular resolution to both sidelines when the aircraft passed over the reference microphone at an altitude of 394 feet. Ensemble averaging of the data recorded directly beneath the flight path is possible using data from the three microphones which form the stem of the "T" and the reference microphone. This microphone array design is useful for measuring the lower hemispherical acoustic characteristics of the test vehicle performing steady state flight operations (constant airspeed, constant glideslope, fixed nacelle angle) as described in Reference 12, and to provide data for code validations.

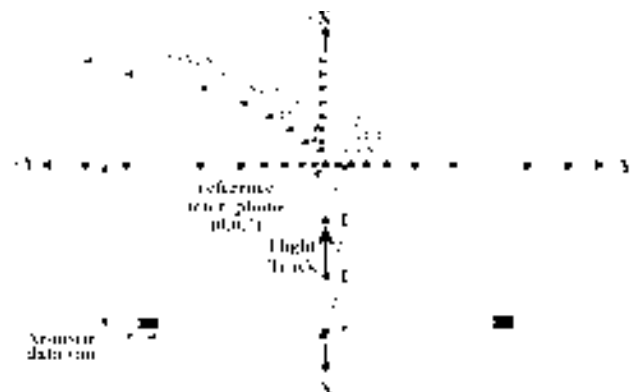


Figure 4. Phase 1 microphone array configuration.

The large microphone array shown in Figure 5 was used during Phase 2. The array consisted of 30 ground

board mounted microphones arranged over a 2000 foot by 7000 foot area. The center of the hover pad was the origin of the coordinate system used during Phase 2 testing. The desired flight track passed directly overhead of the line of microphones located at $Y = 0$, and the typical run terminated in an IGE hover over the hover pad. The acoustic data acquired off the starboard side of the aircraft were folded over to represent measured data off the port side of the aircraft. The assumption that the acoustic radiation pattern is symmetric about the XV-15's longitudinal axis was verified based on examination of the Phase 1 data. This microphone array design is useful for measuring actual ground footprints for any type of tiltrotor flight operations, and is particularly useful for quantification of the acoustic characteristics of a tiltrotor performing highly complex, non-steady state approaches. In addition to the NASA microphones, a DAT recorder acquired data from two Bell microphones that were deployed at $X = -7000$ feet and -8000 feet, as shown in Figure 5. No data from the Bell microphones are presented in this paper.

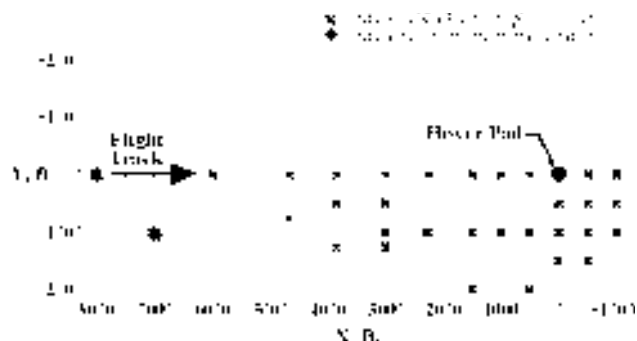


Figure 5. Phase 2 microphone array configuration.

Acoustic Data Processing

The 8-mm tapes containing the digitized acoustic signals were read into DEC Alpha workstations for signal processing at the conclusion of testing each day. Start and stop times were selected at the endpoints in time where all data systems (acoustic, aircraft tracking and state, and weather) were simultaneously acquiring data. The digital acoustic time domain data were transformed to the frequency domain using 8192-point FFTs with a Hamming window, corresponding to 0.4096 second blocks of data. These FFTs were used to compute narrowband spectra, which were directly integrated to obtain Overall Sound Pressure Levels (OASPL). In addition, A-weighting was applied to each spectrum before integration, to provide the A-weighted Sound Pressure Level (L_A) for each time block. These L_A results were then integrated over multiple blocks of data for

cases where computation of Sound Exposure Level (SEL) was desired.

By relating the time-dependent OASPL and L_A acoustic measurements acquired during Phase 1 to the corresponding aircraft position data, effective contours of OASPL and L_A vs. distance were computed using the technique described in Reference 12. The technique for performing this computation is depicted graphically in Figure 6. In Figure 6a, the aircraft flies at a constant operating condition over the linear microphone array, which is perpendicular to the ground track (projection of the flight track on the ground). The 0.4096 second data blocks are related to the aircraft position as shown in Figure 6b, which provides noise levels related to emission angles. By freezing the aircraft at a point in space, these noise directivity data can be projected onto the ground, as shown in Figure 6c, producing a detailed, high resolution noise contour. While the example shown in Figure 6 is for level flight, the same technique can be used when the aircraft is ascending or descending as well. However, because the aircraft's altitude is constantly changing, the projection onto the ground does not represent a "flat earth" ground contour. Instead, the data as measured project onto a plane that is slanted at the same angle as the flight path. This projection can be converted to remove the slant by correcting the measured data at each emission angle for distance and other

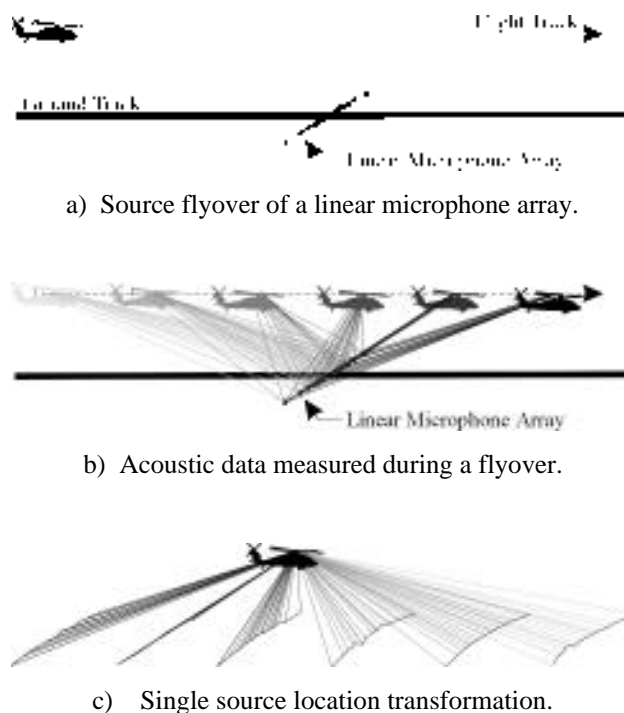


Figure 6. Single source effective surface contour calculation.

propagation changes. However, this has not been done for the Phase 1 contours shown in this paper, which are presented as measured. It should be emphasized that the approach used in Phase 1 is useful only when the aircraft is operated at a constant condition. Otherwise, an array of microphones such as used in Phase 2 is required. In addition to time histories and effective contours, SEL vs. sideline position can be determined, which facilitates comparison of different test conditions.

For Phase 2 data, each noise metric has to be evaluated in the context of a spatial distribution of noise. Primarily, the Phase 2 data have been used to compare SEL noise footprints for different flight approach profiles. Contours of non-integrated metrics, such as L_A , must be considered as “snapshots” in time across the spatial coverage of the Phase 2 microphone array. These snapshots can be useful in assessing the noise generated by the aircraft during a particular portion of the approach, but the noise footprints are better suited for assessing the overall noise impact of various approach profiles.

Results and Discussion

Selected results from both Phase 1 and Phase 2 of the test program are presented in the following sections. These include an assessment of daily repeatability, comparison of results for different operating conditions, and identification of significant changes in noise levels for similar flight conditions.

Data Repeatability

To examine the repeatability of the data obtained during this test program, and as a quick method of verifying the proper operation of all microphone systems, the first run of each flight during Phase 1 was performed at the same operating condition of 90 knots and 60° nacelle angle for a level flyover at 394 feet altitude. These runs are referred to as “housekeeping” runs. Figure 7 presents plots of maximum Overall Sound Pressure Level ($OASPL_{max}$), maximum A-weighted Sound Pressure Level (L_{Amax}), and SEL as functions of sideline position for all housekeeping runs. Figure 7a shows that the highest $OASPL_{max}$ was obtained on the flight path centerline and the levels decrease rapidly with increasing sideline distance with the exception of secondary peaks approximately 400 feet to either side of the centerline. Except for two runs, the $OASPL_{max}$ for all housekeeping runs fall within approximately ± 1.5 dB of the mean level at all measurement locations. Two runs

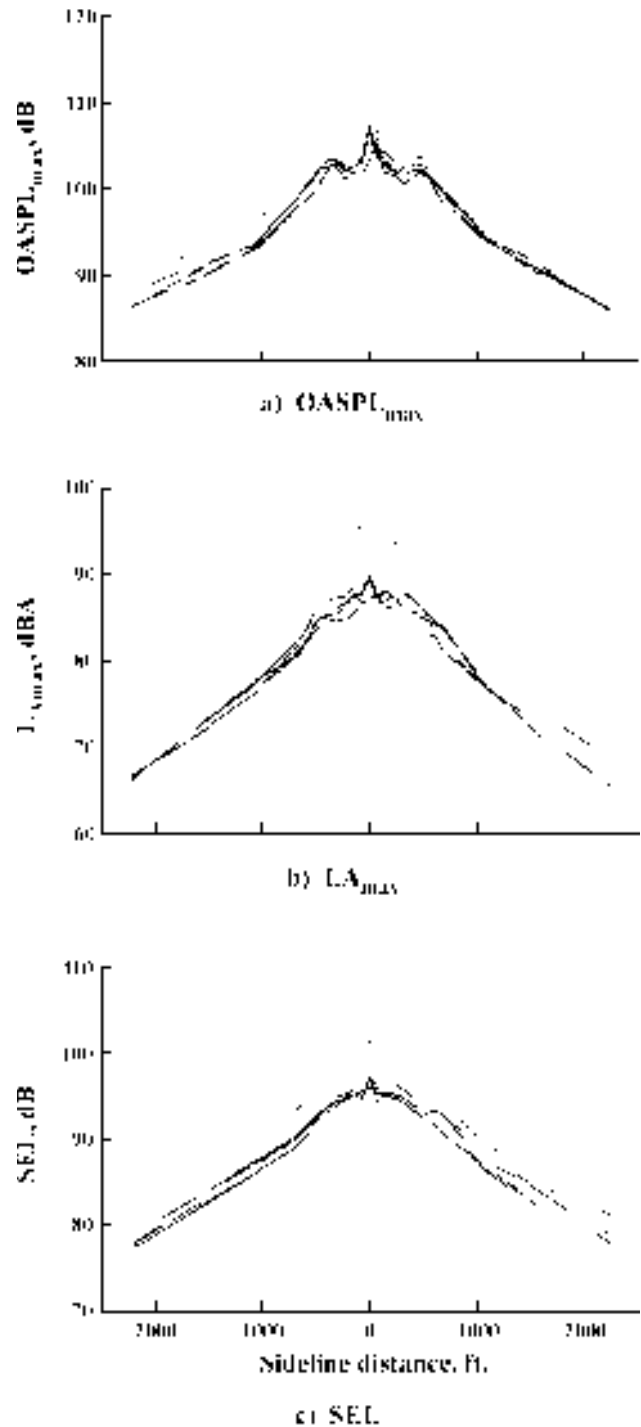


Figure 7. Housekeeping runs; 90 knots, 60° nacelle angle, 394 foot, level flyover.

have levels approximately 4 dB higher than the mean level between -500 and +500 feet of the centerline and are represented in the figure with a dashed and a dotted line. These data were acquired during two flights on Day 8 of the 10 Phase 1 test days and their levels are nearly

equal at all measurement locations except at the centerline. The reason for the difference has not been determined. Similar trends are seen for L_{Amax} and SEL shown in Figures 7b and 7c, with the majority of runs within ± 1.5 dB of the mean level at all measurement locations. However, the differences between the mean levels and the levels obtained on Day 8 are approximately 5 to 8 dBA, depending on the sideline location, for L_{Amax} (Figure 7b). Comparing the differences between the mean levels and the levels obtained on Day 8, the SELs (Figure 7c) show only slightly increased differences near the centerline compared to the $OASPL_{max}$. However, the differences towards the sidelines are about 2 dB greater than those seen for the $OASPL_{max}$.

Phase 1 Approaches

In Figure 8, SEL as a function of the sideline distance for the constant approach conditions of 70 knots and 9° descent angle is presented for nacelle angles of 60° , 70° , 80° , 85° , and 90° . The maximum SEL for each run occurs near the centerline and varies from 100 dB for a 60° nacelle angle to 110 dB for a 90° nacelle angle. In general, the SEL increases with increasing nacelle angle. The difference between the minimum and maximum level for a given sideline distance decreases with increasing sideline distance, from 10 dB near centerline to less than 2 dB 2200 feet to either side. The variation in SEL is somewhat greater to the port side of the aircraft (positive sideline direction) than to the starboard side and is probably due to differences in the actual flight tracks. For the 60° and 70° nacelle angle approaches the actual flight track was substantially off the desired track ($Y = 0$) near the microphone array. When the aircraft passed over the microphone array, the 60° and 70° nacelle angle approaches were -49 feet and -100 feet to the sideline, respectively, while the other approaches were -2, 7, and 17 feet to the sideline. Hence, if these differences in track were taken into account (beyond the scope of the current effort) the noise directivity to the port and starboard sides would be symmetrical.

Figure 9 presents L_A contours for the 60° and 90° nacelle angle approaches of Figure 8, developed using the technique described during the discussion of Figure 6. This figure represents the noise radiated from the XV-15 as if it was frozen in space 394 feet above the point marked with an X on Figure 9. For a 90° nacelle angle (Figure 9a), a significant area just in front of the aircraft is exposed to noise levels above 95 dBA, with a smaller area exposed to levels above 100 dBA. The areas just in front of the aircraft, but to the extreme sidelines, are exposed to levels of about 65 dBA. In comparison, Figure 9b shows a corresponding contour for a matching

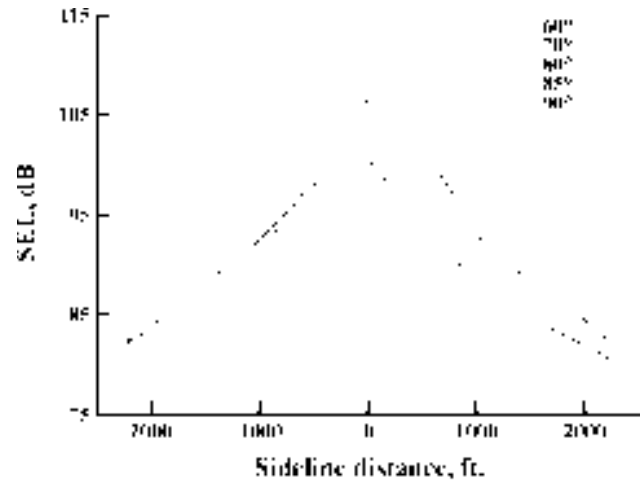


Figure 8. Sound exposure level; 70 knot, 9° approach.

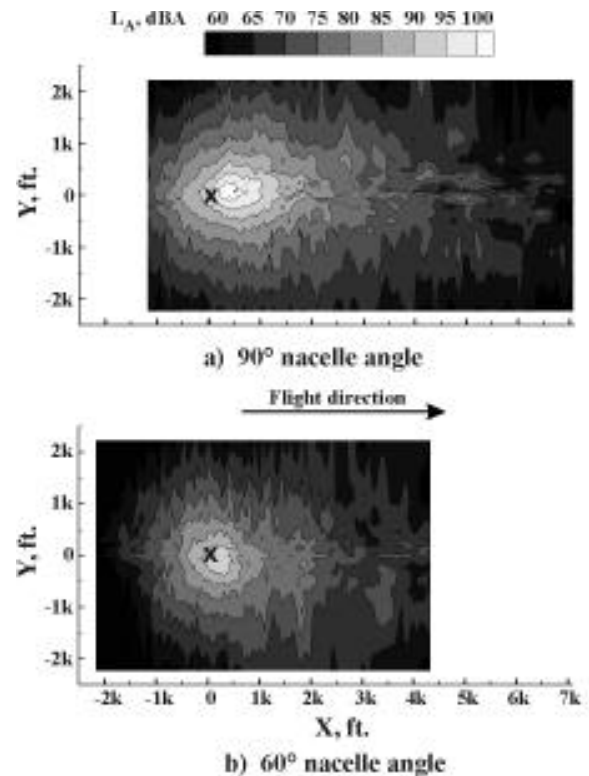


Figure 9. L_A contours; 70 knot, 9° approach.

descent case, except that the nacelles are now at an angle of 60° . Here, there is no region with levels above 95 dBA and only a small region with levels above 90 dBA. For this nacelle angle, the areas just in front of the aircraft, but to the extreme sidelines, are exposed to levels of about 60 dBA. Figures 8 and 9 illustrate the significant noise abatement potential offered by the unique tiltrotor capability of nacelle tilt during approach operations. However, the amount of noise reduction

appears to decrease with increasing sideline distance, as is the case for helicopters using noise abatement procedures (Ref. 13).

Phase 2 Approaches

One method of comparing the Phase 2 runs is to compare the ground contour areas that are exposed to a given noise level. Figure 10 presents the ground area in acres as a function of SEL for 16 different approaches that all ended in an IGE hover over the hover pad. The results of Figure 10 show that the ground area that is exposed to a given noise level can be significantly affected by the type of approach that is performed. For example, the ground area exposed to an SEL of at least 102 dB varied from a minimum of 26.5 acres for approach #1 to a maximum of 104.8 acres for approach #16. The minimum SEL level of 102 dB was selected as this was the minimum level for which all approaches contained a closed contour within the area covered by the Phase 2 microphone array shown in Figure 5. Once measurement effects are taken into account, this would represent a 65 L_{DN} contour for approximately 30 operations per day. The rate at which the area decreases with SEL can also be affected by the type of approach. For example, while approach #1 has a slightly smaller ground area exposed to at least 102 dB compared to approach #2, the area exposed to at least 106 dB is almost seven times larger for approach #1 (9.4 acres vs. 1.4 acres).

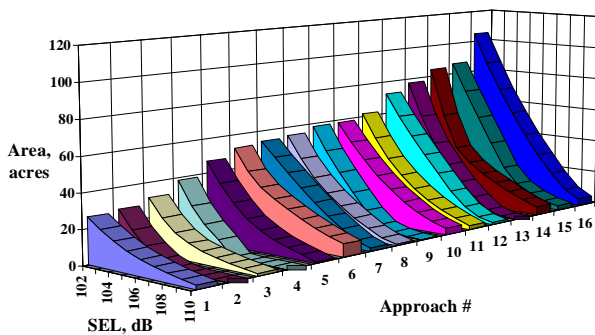


Figure 10. Contour area as a function of SEL for 16 different approach profiles.

Characteristics of the SEL ground contours for a “quiet” approach (approach #2), a “normal” approach (approach #8), and a “loud” approach (approach #16) are presented in Figure 11. A normal approach is defined as the type of approach that the pilot would fly without intentionally flying noise abatement procedures. In the figure, the aircraft is approaching on centerline ($Y = 0$) from the $-X$ direction and the approach terminates in an IGE hover over the hover pad located at $X = Y = 0$. The

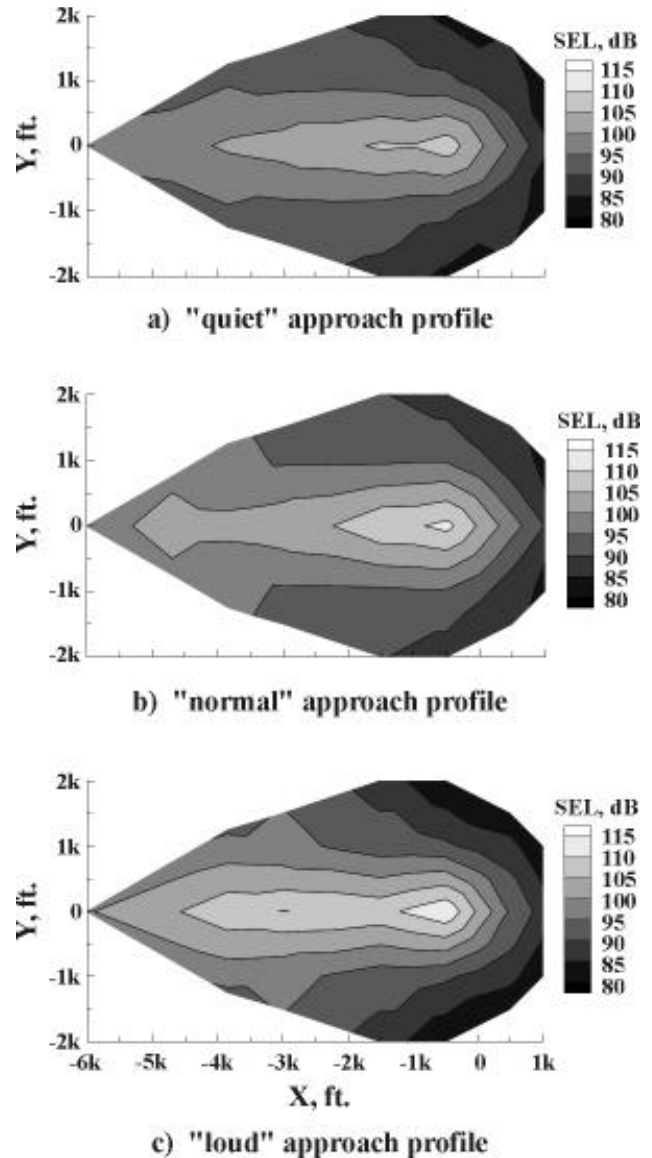


Figure 11. SEL ground contours.

area of maximum level does not contain the area about the hover pad (as would be expected) due to a combination of the microphone distribution and the linear interpolation technique between the measurement locations used by the graphics software. For safety reasons, a microphone could not be located on the hover pad. Because of this, the maximum levels were measured at the microphone located at $X = -500$ feet. The next measurement location was located at $X = +500$ feet, and the levels decrease rapidly forward of the hover pad. The maximum SEL measured for the quiet approach (Figure 11a) is 107 dB while the maximum SEL measured for the normal approach (Figure 11b) was 111.5 dB and for the loud approach (Figure 11c) was 114 dB. Comparing the quiet and the normal approaches, the normal

approach contours appear to be larger for all levels, with the differences being more pronounced at the higher levels. Comparing the normal approach and the loud approach, significant differences are seen in the size of most contour levels. The contour areas for the 110, 105, and 100 dB levels are much larger for the loud approach, while the 95 dB contour areas are about the same. Within the measurement region, the 90 dB and 85 dB contours are closer to the landing pad area for the loud approach than for both the normal and quiet approaches. This indicates that while this type of approach is louder in most regions, it appears to be somewhat quieter further out in front and to the sides of the landing point. However, this result is not significant, since the noise levels forward of and around the landing pad would be dominated by the length of time spent in hover rather than by the approach profile during actual aircraft operations.

Examination of all the Phase 2 approach noise contours indicate significant differences in the shapes of the various contour levels. While high noise contour regions for some approaches are quite long along the flight path and roll off quickly to the sidelines, other approaches have much shorter and wider high noise regions. Such differences indicate that there will most likely not be a single approach profile deemed to be “the quietest” for all situations. Rather, an optimum profile will have to be selected for each individual landing site based on population distributions or some other impact criteria.

Figure 12 shows the aircraft operating conditions of altitude, airspeed, and nacelle angle as a function of the up-range distance from the hover pad for the quiet, normal, and loud approaches discussed in the previous paragraph. Comparison of the altitude for the quiet and loud approaches (Figure 12a) shows that the quiet approach begins at a higher altitude and transitions from level flight to an approximately fixed descent angle sooner than the loud approach. The descent angle for the quiet approach is approximately 1.6° steeper (6.7° vs. 5.1°) than for the loud approach. The descent angle for the normal approach is slightly steeper than that for the quiet approach. Unfortunately, the aircraft state and tracking data for the normal approach does not begin until the aircraft is only about 7000 feet up-range compared to 14,000 to 15,000 feet up-range for the quiet and loud approaches, so the flight conditions for the normal approach prior to reaching the 7000 foot up-range point are not known.

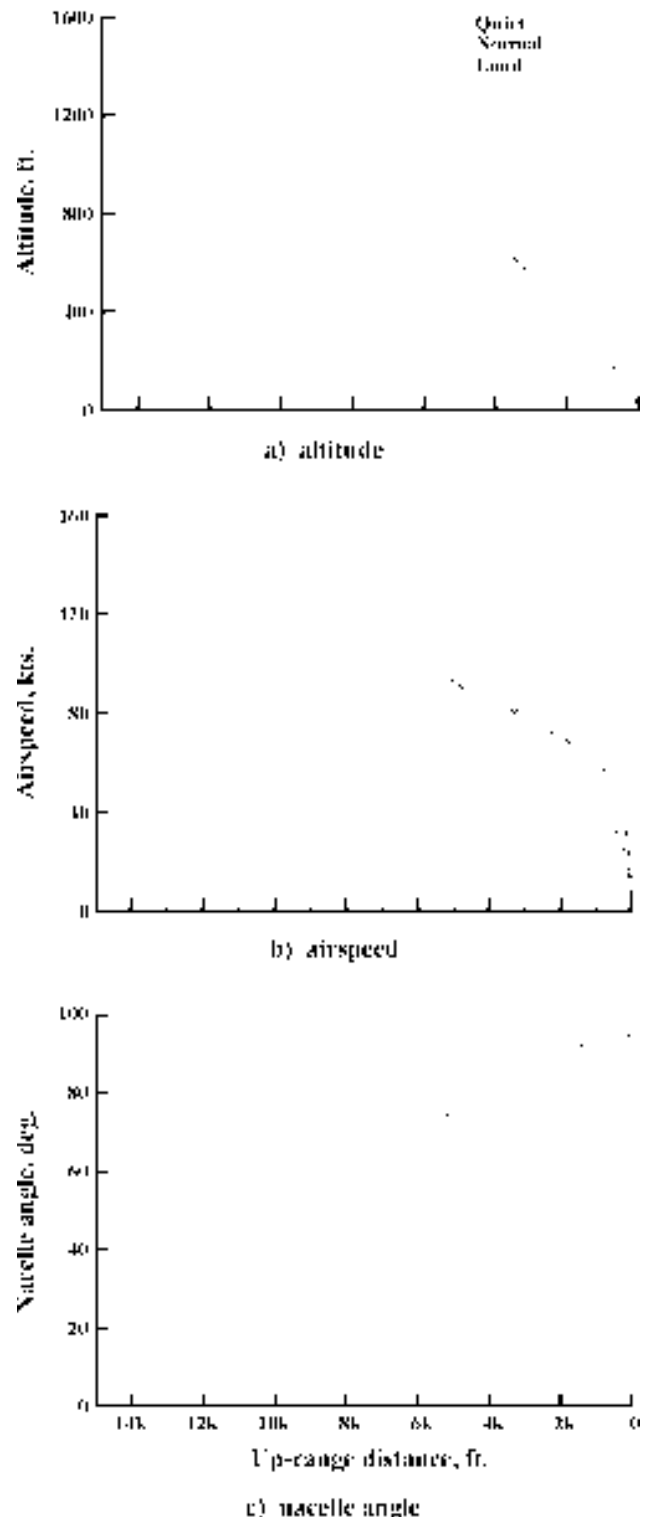


Figure 12. Approach conditions.

Comparison of the airspeed for the three approaches (Figure 12b) shows that the quiet approach began at a slightly higher airspeed than the loud approach, but quickly decelerated to a lower airspeed between about

12,000 and 4000 feet out, then transitioned again to a slightly higher airspeed to the hover pad. Hence, the quiet approach had a slightly higher deceleration rate near the hover pad. The airspeed for the quiet approach is slightly lower than for the normal approach throughout the entire approach profile.

Comparison of the nacelle angles (Figure 12c) show that, over the up-range distance for which the noise generated will provide the dominant contribution to the Figure 11 SEL contours, the quiet and normal approaches are made at nacelle angles 5° to 20° below the vertical (90°) over most of the approach path. Meanwhile, the loud approach had converted to nacelle angles greater than 85° while still approximately 4500 feet up-range.

Phase 2 Takeoffs

Figure 13 presents the SEL ground contour for a typical takeoff condition. The shading for the SEL contour levels are the same as in Figure 11. The maximum SEL for this takeoff is 102 dB and the area of the 102 dB SEL contour is 0.17 acres. During this takeoff run, the XV-15 was completely converted to airplane mode (0° nacelle angle) at approximately 3400 feet from the hover pad. At this point the aircraft altitude was about 180 feet and the airspeed was about 125 knots. When the 102 dB SEL contour is examined for all takeoff conditions, the maximum takeoff contour area measured was 2.2 acres whereas the minimum area on approach for the 102 dB SEL contour was 26.5 acres. These results indicate that the noise levels produced by the XV-15 during takeoff are substantially lower than for approach conditions and should not be considered as a significant problem.

Concluding Remarks

Acoustic measurements were obtained for the XV-15 tiltrotor aircraft operating at a wide range of flight conditions in a two-phase test effort. In Phase 1, the microphone array was linear and perpendicular to the flight path, and the XV-15 was operated at steady state conditions during the entire flyover for each data run. Results from Phase 1 show up to 10 dB reduction in SEL due to reducing nacelle angle from 90° to 60° while maintaining a constant airspeed and glideslope. In addition, good repeatability, typically within ± 1.5 dB, was found for matching flight conditions, and the noise radiation pattern is symmetric about the centerline of the aircraft, as would be expected. In Phase 2, the

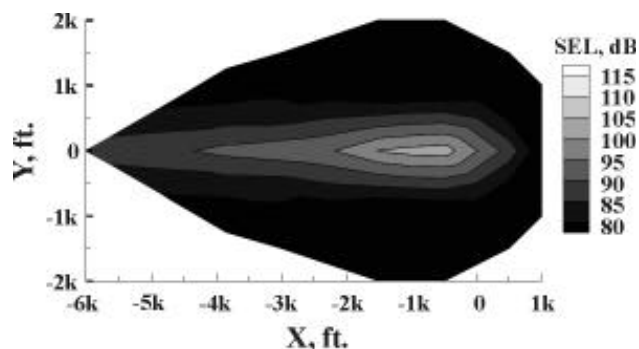


Figure 13. SEL contour for a typical takeoff condition.

microphone array was distributed over a wide area, to directly measure the noise footprint of the XV-15 during different flight approach and takeoff profiles. Results from Phase 2 show that the ground area exposed to a particular noise level is significantly affected by the type of approach that is performed. For the XV-15's 102 dB SEL contour, an impacted area of 104.8 acres was reduced to 26.5 acres by flight procedure modifications. This would represent a 65 L_{DN} contour for a nominal 30 operations per day. In addition, approach procedures can be varied to "tailor" the noise footprint shape to individual vertiports. Some procedures produce long thin contours, while others produce shorter, wider contours. Finally, the takeoff condition has only a secondary effect on the total noise of tiltrotor operations, impacting land areas which are an order of magnitude less than those impacted during approach. For the XV-15's 102 dB SEL contour, less than 2.2 acres were impacted during the loudest takeoff, compared with 26.5 acres for the quietest approach.

Acknowledgments

The authors would like to recognize the efforts of all of the personnel involved with the test program from Bell Helicopter Textron, Inc., NASA Ames and Langley Research Centers, the U. S. Army, and the associated contractors affiliated with these organizations. Without the extreme dedication of all of the people involved with the test program, the test would not have been a success. However, a few individuals and groups deserve special recognition for their efforts. These include Colby Nicks and Bill Martin of Bell for their work with the XV-15, the field measurement team from Wyle Labs for always having the acoustic measurement systems ready for testing, and Jaye Moen of NASA Langley for keeping the weather balloon aloft on demand. In particular, Ken Rutledge and Mark Wilson, both formerly of Lockheed Martin Engineering and Sciences Co., deserve an enormous amount of credit for processing all of the

acoustic data acquired during this test program while on-site, as well as assimilating all of the different types of data into one comprehensive data set. This paper would have been impossible without their efforts.

References

1. Huston, R., Golub, R., and Yu, J., "Noise Considerations for Tiltrotors," AIAA Paper No. 89-2359, 1989.
2. "Civil Tiltrotor Development Advisory Committee Report to Congress," Volume 1 Final Report, Dec. 1995.
3. George, A., Smith, C., Maisel, M., and Brieger, J., "Tilt Rotor Aircraft Aeroacoustics," Presented at the American Helicopter Society 45th Annual Forum, Boston, MA, May 22-24, 1989.
4. Lee, A., and Mosher, M., "An Acoustical Study of the XV-15 Tilt Rotor Research Aircraft," AIAA Paper No. 79-0612, 1979.
5. Maisel, M., and Harris, D., "Hover Tests of the XV-15 Tilt Rotor Research Aircraft," AIAA Paper No. 81-2501, 1981.
6. Conner, D., and Wellman, J., "Hover Acoustic Characteristics of the XV-15 with Advanced Technology Blades," AIAA Journal of Aircraft, Volume 31, Number 4, July-August 1994.
7. Brieger, J., Maisel, M., and Gerdes, R., "External Noise Evaluation of the XV-15 Tilt Rotor Aircraft," Presented at the AHS National Technical Specialists' Meeting on Aerodynamics and Aeroacoustics, Arlington, TX, February 25-27, 1987.
8. Edwards, B., "XV-15 Tiltrotor Aircraft Noise Characteristics," Presented at the American Helicopter Society 46th Annual Forum, Washington, DC, May 21-23, 1990.
9. Marcolini, M., Conner, D., Brieger, J., Becker, L., and Smith, C., "Noise Characteristics of a Model Tiltrotor," Presented at the American Helicopter Society 51st Annual Forum, Fort Worth, TX, May 9-11, 1995.
10. "Tilt Rotor Research Aircraft Familiarization Document," NASA TMX-62,407, Jan. 1975.
11. Gray, D., Wright, K., and Rowland, W., "A Field-Deployable Digital Acoustic Measurement System," Presented at Technology 2000 (Proceedings published as NASA CP 3109, Vol. 2.), Washington, DC, Nov. 27-28, 1990.
12. Wilson, M., Mueller, A., and Rutledge, C., "A New Technique for Estimating Ground Footprint Acoustics for Rotorcraft Using Measured Sound Fields," Presented at the American Helicopter Society Vertical Lift Aircraft Design Conference, San Francisco, CA, Jan. 18-20, 1995.
13. Yoshikami, S., "Flight Operations Noise Tests of Eight Helicopters," FAA-EE-85-7, Aug. 1985.